

Surface plasmon polaritons in double-walled carbon nanotubes

© S.A. Afanas'ev¹, V.A. Zaitsev¹, S.G. Moiseev^{1,2}, I.A. Rozhleys¹, D.G. Sannikov^{1,¶}, G.V. Tertyshnikova¹

¹ Ulyanovsk State University,
432970 Ulyanovsk, Russia

² Kotelnikov Institute of Radio Engineering and Electronics (Ulyanovsk Branch), Russian Academy of Sciences,
432071 Ulyanovsk, Russia

¶ E-mail: sannikov-dg@yandex.ru

Received April 27, 2024

Revised July 4, 2024

Accepted October 30, 2024

The dispersion characteristics of surface plasmon polaritons in double-walled carbon nanotubes have been studied, taking into account ohmic losses. A dispersion equation in matrix form is obtained for the surface plasmon polaritons, taking into account the anisotropy of the electrical conductivity of nanotube walls. Its numerical solutions are found for low-order plasmonic modes propagating over a wide frequency range (including THz and visible range). It was found that for double-walled carbon nanotubes of sufficiently large radii, the surface plasmon polaritons deceleration coefficient can exceed 300.

Keywords: carbon nanotube, surface plasmon polaritons.

DOI: 10.61011/SC.2024.09.59910.6326A

1. Introduction

Surface plasmon polaritons (SPPs) are electromagnetic excitations at the dielectric-conductor interface, confined in the perpendicular direction and resulting from the interaction of electromagnetic fields with fluctuations in the electronic plasma of the conductor [1]. Carbon nanotubes (CNTs) represent a promising class of structures that can serve to excite SPPs [2]. CNTs can be single- or multi-walled (MWCNTs) and exhibit both metallic and semiconductor properties. When the phase velocity of the slow SPPs and the drift velocity of the charge carriers on the walls of the CNT are comparable in magnitude and coincide in direction, then the drift current can amplify the SPP wave [3]. It was proposed in paper [4] to use this effect in a terahertz radiation generator circuit based on an array of parallel double-walled CNTs (DWCNTs) with direct current flow. In this regard, a critical task is to investigate the conditions of excitation of slow high-quality SPPs on CNT walls.

The dispersion properties of SPPs in DWCNTs are studied in this paper, taking into account the anisotropy of the electrical conductivity of the walls and ohmic losses, and the deceleration coefficient of SPP modes in CNTs of different radii is analyzed. The plasmonic properties of nanotubes are described within the framework of the hydrodynamic approach [5,6].

2. DWCNT conductivity model

The DWCNT is modeled by a system of two coaxial cylindrical walls made of graphene with radii a_1 and a_2 ($a_2 > a_1$) separated by a typical interlayer distance of 0.34 nm within the framework of the linearized hydrodynamic theory developed in relation to CNT [5]. The conductivity tensor CNT $\hat{\sigma}_j$ ($j = 1, 2$ — wall number) was derived in the article [6], using the hydrodynamic model, which determines the surface

current density. The equations of motion of charge carriers and the equation of continuity, were used for deriving it. Including losses, the components of the conduction tensor in cylindrical coordinates (r, φ, z) are expressed as:

$$\begin{aligned}\sigma_{zz}^{jm} &= \sigma_0 \Omega^{-1} \left(\omega \tilde{\omega} - \frac{\alpha m^2}{a_j^2} \right), \\ \sigma_{z\varphi}^{jm} &= \sigma_{\varphi z}^{jm} = \sigma_0 \Omega^{-1} \frac{\alpha q m}{a_j}, \\ \sigma_{\varphi\varphi}^{jm} &= \sigma_0 \Omega^{-1} (\omega \tilde{\omega} - \alpha q^2),\end{aligned}\quad (1)$$

where $\sigma_0 = in_0 e^2 / (m_{\text{eff}} \tilde{\omega})$, n_0 is the equilibrium surface electron density on the walls of the nanotube, e and m_{eff} are the electron charge and effective mass, $\Omega = \omega \tilde{\omega} - \alpha (q^2 + \frac{m^2}{a_j^2})$, $\tilde{\omega} = \omega + i\tau^{-1}$, q is the SPP propagation constant, τ is the electron relaxation time, m is the azimuthal mode number for SPP-mode, parameter $\alpha = \frac{V_F^2}{2}$ is related to spatial dispersion (the components of the tensor $\hat{\sigma}_j$ depend on q), V_F is Fermi velocity. A special feature of this model is the inclusion of the azimuthal components of the surface current density on the nanotube walls, as well as the dependence of conductivity on the azimuthal mode number.

3. The dispersion relation for SPP in the DWCNT

Using Maxwell's system of equations, in the general case of hybrid modes ($E_z, H_z \neq 0$), the Helmholtz equation for the longitudinal components of electric E_z and magnetic H_z fields can be written as follows:

$$\frac{d^2 E_z}{dr^2} + \frac{1}{r} \frac{dE_z}{dr} - \left(\kappa^2 + \frac{m^2}{r^2} \right) E_z = 0,$$

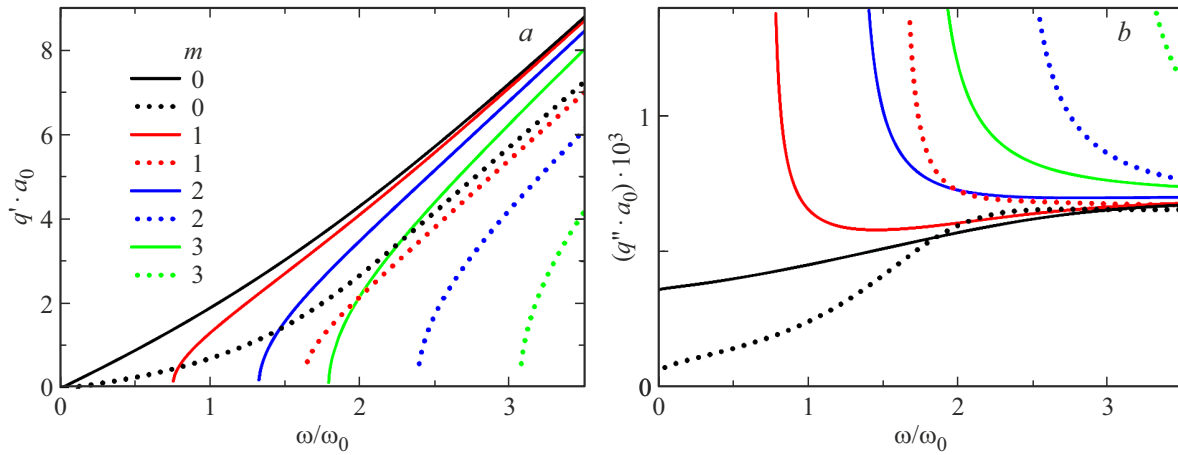


Figure 1. Dispersion relations for SPPs in the DWCNT with parameters $a_1 = 0.5$ nm, $a_2 = 0.84$ nm (solid lines — LF branches, dotted lines — HF branches). Relaxation time $\tau = 10^{-12}$ s [7], $a_0 = 1$ nm, $\omega_0 = 2.3 \cdot 10^{15}$ c^{-1} . (A color version of the figure is provided in the online version of the paper).

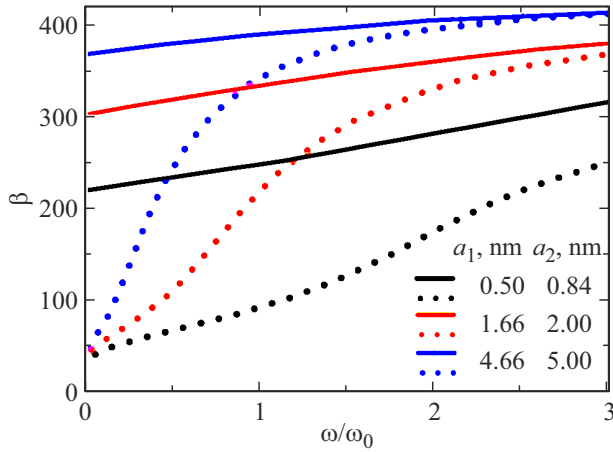


Figure 2. Frequency dependences of the deceleration coefficient $\beta = \frac{c}{v_{ph}}$ of the fundamental mode ($m = 0$) for DWCNTs of various radii (solid lines — LH branches, dotted lines — HF branches). Parameters are the same as in Figure 1.

$$\frac{d^2 H_z}{dr^2} + \frac{1}{r} \frac{dH_z}{dr} - \left(\kappa^2 + \frac{m^2}{r^2} \right) H_z = 0, \quad (2)$$

where $\kappa^2 = q^2 - \omega^2/c^2$ is the square of the transverse wavenumber, c is the speed of light in a vacuum. The values of q and κ are real in the absence of losses, while $q > \omega/c$, which indicates SPP mode deceleration. Solving equations (2) with appropriate boundary conditions yields the following dispersion relation for SPPs:

$$\det \begin{pmatrix} I_m(\kappa a_1) \Pi_{z\phi}^{(1)} & 0 & -M_{14} + \frac{i\omega\mu_0}{\kappa} I'_m(\kappa a_1) \sigma_{\phi\phi}^{1m} & M_{14} \\ \frac{I_m(\kappa a_1) K_m(\kappa a_2)}{K_m(\kappa a_1)} \Pi_{z\phi}^{(2)} & M_{22} & \frac{i\omega\mu_0}{\kappa} \frac{I'_m(\kappa a_1) K'_m(\kappa a_2)}{K'_m(\kappa a_1)} \sigma_{\phi\phi}^{2m} & M_{24} \\ -M_{32} - I_m(\kappa a_1) \Pi_{zz}^{(1)} & M_{32} & -M_{34} - \frac{i\omega\mu_0}{\kappa} I'_m(\kappa a_1) \sigma_{z\phi}^{1m} & M_{34} \\ -\frac{I_m(\kappa a_1) K_m(\kappa a_2)}{K_m(\kappa a_1)} \Pi_{zz}^{(2)} & M_{42} & -\frac{i\omega\mu_0}{\kappa} \frac{I'_m(\kappa a_1) K'_m(\kappa a_2)}{K'_m(\kappa a_1)} \sigma_{z\phi}^{2m} & M_{44} \end{pmatrix} = 0, \quad (3)$$

where I_m and K_m are modified Bessel functions of m -th order,

$$\Pi_{z\phi}^{(j)} = \sigma_{z\phi}^{jm} + \sigma_{\phi\phi}^{jm} \frac{mq}{\kappa^2 a_j}, \quad \Pi_{zz}^{(j)} = \sigma_{zz}^{jm} + \sigma_{z\phi}^{jm} \frac{mq}{\kappa^2 a_j},$$

$$M_{22} = K_m(\kappa a_2) \Xi \Pi_{z\phi}^{(2)}, \quad M_{32} = -\frac{i\omega\epsilon_0}{\kappa^2 a_1 K_m(\kappa a_1)},$$

$$M_{42} = -M_{32} - K_m(\kappa a_2) \Xi \Pi_{zz}^{(2)},$$

$$M_{14} = -\frac{1}{\kappa a_1 K'_m(\kappa a_1)},$$

$$M_{24} = -\frac{1}{\kappa a_2 K'_m(\kappa a_2)} + \frac{i\omega\mu_0}{\kappa} \Gamma K'_m(\kappa a_2) \sigma_{\phi\phi}^{1m},$$

$$M_{34} = \frac{mq}{\kappa^2 a_1} M_{14},$$

$$M_{44} = \frac{mq}{\kappa^3 a_2^2 K'_m(\kappa a_2)} - \frac{i\omega\mu_0}{\kappa} \Gamma K'_m(\kappa a_2) \sigma_{z\phi}^{2m},$$

$$\Xi = \frac{I_m(\kappa a_2)}{K_m(\kappa a_2)} - \frac{I_m(\kappa a_1)}{K_m(\kappa a_1)},$$

$$\Gamma = \frac{I'_m(\kappa a_2)}{K'_m(\kappa a_2)} - \frac{I'_m(\kappa a_1)}{K'_m(\kappa a_1)}.$$

It is known that the dispersion relation has N different positive roots for each m for SPPs in MWCNT having N walls [6]. In particular, the solution of the equation (3) splits into two branches for DWCNT — high frequency (HF) and low frequency (LF) branches.

4. Numerical analysis and discussion

The dispersion equation (3) was solved numerically with respect to the complex propagation constant $q = q' + iq''$. Figure 1 shows the dependences of the values $q'a_0$ and

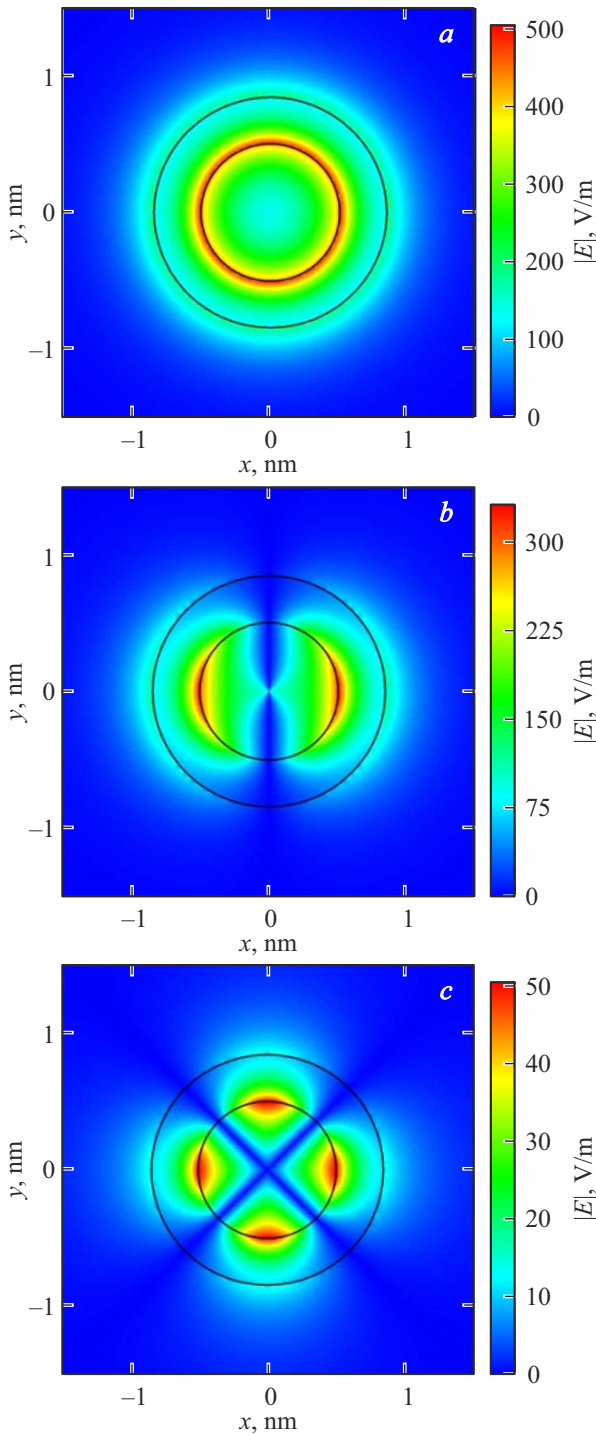


Figure 3. Distribution of the electric field modulus for HF branches with $m = 0$ (a), 1 (b) and 2 (c) in the cross-section of the DWCNT at the reduced frequency $\omega/\omega_0 = 2.5$. The other parameters are the same as in Figure 1. (A color version of the figure is provided in the online version of the paper).

$q''a_0$ on the reduced frequency ω/ω_0 for the four lower SPP modes in the DWCNT based waveguide. The following normalization factors are used: $a_0 = 1$ nm, $\omega_0^2 = e^2 n_0 / \epsilon_0 m_{\text{eff}} a_0$. The following estimate is obtained for the ratio of the equilibrium surface electron density to the effective mass of charge carriers in [8] which is a part of the last expression: $\frac{n_0}{m_{\text{eff}}} = \frac{2V_F}{\pi^2 \hbar a_0}$, where the value of the Fermi velocity for metallic CNT is estimated as $V_F \approx 10^6$ m/s. This gives the value $2.3 \cdot 10^{15} \text{ c}^{-1}$ for the parameter ω_0 .

In the spectral region $\omega < 0.74\omega_0$, there is a weakly attenuating mode with the index $m = 0$, while for its LF-branch the dependence $q'(\omega)$ is close to linear. The attenuation coefficient q'' of the mode with the index $m = 0$ remains below $4 \cdot 10^5 \text{ m}^{-1}$ in the region $\omega < \omega_0$, which corresponds to a path length of the order of several μm . Higher-order modes ($m \geq 1$) exhibit significantly greater attenuation than the fundamental mode in the frequencies of the cutoff, where $q' \ll q''$.

Figure 2 shows the frequency dependences of the deceleration coefficient $\beta = \frac{c}{V_{\text{ph}}}$ (V_{ph} is the phase velocity of the SPP) of the fundamental mode in DWCNTs of varying radii a_j . It can be seen that the value β is higher for the LF branch than for the HF branch, and this value increases with the increase of the nanotube radius. The frequency dependence of the parameter β is weakly expressed for the LF branch. Values of $\beta > 300$ are achieved at all frequencies for this branch, in the case of large-radius nanotubes, which makes it possible to realize the phase synchronism condition and amplify the surface wave due to interaction with drift currents.

Figure 3 shows the electric field modules in the DWCNT cross section for the first three modes ($m = 0, 1, 2$) corresponding to the HF branches in Figure 1. It can be seen from the figure that the electric field of the SPP mode is localized mainly on the DWCNT wall of a smaller radius. The field intensity decreases rapidly outside the outer wall of the DWCNT. The maximum value of the modulus of the SPP electric field in the DWCNT decreases with an increase of the azimuthal mode number m .

5. Conclusion

This study demonstrates the existence of SPPs in a DWCNT with a strong localization of radiation inside a nanotube and with a wavelength of several micrometers. The strong localization of the wave field is accompanied by a significant decrease in the phase velocity of the fundamental SPP mode: depending on the diameter of DWCNT, the deceleration coefficient reaches values of 200 and higher. Such a high deceleration of surface waves can be used to implement decelerating systems with high efficiency of converting current pumping energy into SPP energy.

The results obtained in this work for a single nanotube are applicable to sparse arrays of DWCNT. Indeed, for frequencies of the order of 10^{15} c^{-1} , the localization region of the electric field can be estimated by the value of $\kappa^{-1} \approx (q')^{-1} \approx 1$ nm; this means that the considered

DWCNT practically do not affect each other at a distance of more than 4 nm between their walls. Therefore, the results of the study can be useful for the design of deceleration systems based on both single nanotubes and arrays of CNTs.

Funding

This study was supported by the Russian Science Foundation (project No. 23-19-00880).

Conflict of interest

The authors declare that they have no conflict of interest.

References

- [1] S.A. Maier. *Plasmonics: Fundamentals and Applications* (Springer, N. Y., 2007) p. 21. DOI: 10.1007/0-387-37825-1
- [2] G.Y. Slepyan, S.A. Maksimenko, A. Lakhtakia, O. Yevtushenko, A.V. Gusakov. *Phys. Rev. B*, **60** (24), 17136 (1999). DOI: 10.1103/PhysRevB.60.17136
- [3] A.S. Kadochkin, S.G. Moiseev, Y.S. Dadoenkova, V.V. Svetukhin, I.O. Zolotovskii. *Opt. Express*, **25** (22), 27165 (2017). DOI: 10.1364/OE.25.027165
- [4] S.A. Afanas'ev, A.A. Fotiadi, A.S. Kadochkin, E.P. Kitsyuk, S.G. Moiseev, D.G. Sannikov, V.V. Svetukhin, Y.P. Shaman, I.O. Zolotovskii. *Photonics*, **10** (12), 1317 (2023). DOI: 10.3390/PHOTONICS10121317
- [5] T. Stöckli, J.M. Bonard, A. Châtelain, Z.L. Wang, P. Stadelmann. *Phys. Rev. B*, **64** (11), 115424 (2001). DOI: 10.1103/PhysRevB.64.115424
- [6] A. Moradi. *Appl. Phys. A: Mater. Sci. Process.*, **113** (1), 97 (2013). DOI: 10.1007/s00339-013-7854-5
- [7] R.A. Jishi, M.S. Dresselhaus, G. Dresselhaus. *Phys. Rev. B*, **48** (15), 11385 (1993). DOI: 10.1103/PhysRevB.48.11385
- [8] G. Miano, F. Villone. *IEEE Trans. Ant. Prop.*, **54** (10), 2713 (2006).

Translated by A.Akhtyamov